ResearchGate

See discussions, stats, and author profiles for this publication at: https://www.researchgate.net/publication/329565456

An Efficient Retinal Blood Vessel Segmentation using Morphological Operations

Conference Paper · October 2018

DOI: 10.1109/ISMSIT.2018.8567239

CITATIONS
0

READS
342

4 authors, including:

Umut Özkaya
Selcuk University
26 PUBLICATIONS **22** CITATIONS

SEE PROFILE

Şaban Öztürk
Amasya University
26 PUBLICATIONS **60** CITATIONS

SEE PROFILE

Levent Seyfi
Konya Technical University
52 PUBLICATIONS **115** CITATIONS

SEE PROFILE

Some of the authors of this publication are also working on these related projects:

NOISE REDUCTION IN GPR B-SCAN IMAGES View project

Glass defect detection View project

All content following this page was uploaded by Umut Özkaya on 25 December 2018.

The user has requested enhancement of the downloaded file.

An Efficient Retinal Blood Vessel Segmentation using Morphological Operations

U. Ozkaya[1]*, Ş. Ozturk[2], , B. Akdemir[1] and L. Seyfi[1]
[1]*Konya Technical University/Electrical and Electronics Engineering, Konya, Turkey*
[2]*Amasya University/Electrical and Electronics Engineering, Amasya, Turkey*
**Corresponding Author E-mail: uozkaya@selcuk.edu.tr*

***Abstract*— The structure of retinal vessel carries information about many diseases. It is difficult to analyze this complex structure by human eye. Additionally, it has time-consuming process. In this study, an extremely lower complex and more successful retinal blood vessel segmentation method is proposed via using morphological operators. Colorful retinal images are divided into red, green and blue channels. Green channel is preferred for segmentation on the account of including clear details about retinal vessels. Then, adaptive threshold with 5x5 Gaussian window is applied in order to obtain clean vessel geometry. In the next step, retinal image is sharpened and then, 3x3 wiener filter is applied to it. After wiener filter, some noise in the image decreases but retinal image pixels soften. Therefore, Otsu thresholding is applied to softened images. Finally, morphological operation is performed on gray level images. The proposed method is implemented on test images in DRIVE database. The process time of our method is 0.7-0.8 second and it is faster than other methods. 95,61% accuracy, 85.096% sensitivity and 96.33% specificity rates are obtained.**

***Index Terms*— Biomedical image processing, image texture analysis, image denoising, image edge detection, image segmentation.**

I. INTRODUCTION

The retinal blood vessels are one of the most important part of human visual system. Width and curves of retinal blood vessel can carry symptoms about many diseases. Structure of retinal blood vessels is analyzed in order to be diagnosed such as age-related macular degeneration (AMD), diabetic retinopathy (DR), glaucoma, hypertension and arteriosclerosis [1]. DR is top of the blinding disease list in working-age community [2]. All over the world, about 415 million people at any age have diabetes and also it is envisaged to reach 642 million people by 2040 in accordance with statistics from International Diabetes Federation (IDF) [3]. Blindness ratio caused by DR will rise up year by year. Thus, computer-aided automatic segmentation design with high accuracy has great importance for retinal vessel.

Detection of deterioration in the retinal blood vessel is very critical importance for early diagnosis [4]. Evaluation of retinal images by human eye is time-consuming process because they have more complexity and noise. Also, success of the diagnosis can be changed depending on optomologist experiences [5]. Computer aided diagnosis (CAD) system is used for objective evaluation and fast decision. Retinal images are obtained by using a fundus camera to be assessed by computer software CAD system is performed.

In unsupervised approaches, retinal vessel structure was reconstructed by morphological filters responses which was combined with centerlines of vessel extraction [6]. Lam et al. used a multi-concavity modelling for retinal vessel profile [7]. An active contour model was proposed for retinal blood vessel detection by Al-Diri et al. [8]. Locally adaptive derivative filter on orientation scores (LAD-OS) approach was performed on DRIVE Retinal datasets by Roychowdhury et al. [9]. Nguyen et al. proposed a multi-scale line detection method combined with various scale line response [10]. Self-Organizing Maps (SOM) and Otsu's method was implemented for vessel segmentation by Zhang et al. [11]. Retinal vessel map was detected by feature vectors which were extracted by B-COSFIRE filters [12].

On the other hand, supervised techniques generally give a better results than unsupervised techniques owing to training process. Niemeijer et al. suggested a derivatives of Gaussian matched filters with k-Nearest Neighbor algorithm [13]. Features of retinal blood vessels were extracted by using Gabor filter bank for Bayesian classifier [14]. Artificial neural network was proposed for detection of vasculature by Marín et al. [15]. You et al. tried to detect some types of blood vessels using semi-supervised method based on radial projection [16]. Boosted and bagged decision trees were proposed for segmenting blood vessel by Fraz et al. [17]. Retinal blood vessel images were segmented by means of a cross modality learning algorithm [18].

In the literature, most of proposed methods need many training data sets or long processing time for retinal image segmentation. Also, most of them involves segmentation failure for blood vessel geometry. In this case, sensitivity value is lower. The proposed algorithm operates automatically without any training data. So, it is an unsupervised method that is used for extraction retinal vessel. It has low complexity and low processing time due to using simple morphological methods. Segmented vessel geometry includes a very uniform and high sensitivity rate.

In this study, proposed methodology consists of adaptive thresholding using Gauss windows, image sharpening, image denoising with Weiner filter, Otsu thresholding, morphological opening and circle removing. The rest of the study is designed as follows; Section II describes block diagram of the proposed algorithm and implementation details. Accuracy, sensitivity and specificity rates of proposed and other methods are given in Section III. Conclusion is mentioned in Section IV.

978-1-5386-4184-2/18/$31.00 ©2018 IEEE

II. PROPOSED METHOD

In the proposed method, retinal blood vessels are determined by examining statistical properties of the image. But, retinal images are quite noisy. These noise make it difficult to detect blood vessels. Because, noise distort image statistics. In addition, thin capillaries and retinal image background create challenges. When retinal image structure is examined, these images consist of three different color bands named as Red, Green and Blue. Blue band does not contain much information about blood vessels, red band has much noise and green band has less noise and it has more clearly blood vessels. So, green band is used in this study.

Retinal images are generally divided into two classes as white and black in order to make more meaningful for human. Noise disrupts this process and they are labeled as white. To avoid this situation, noise must be removed. Noise removal process should be done in small steps. Because thin blood vessels can be perceived as background noise. If they are perceived as background noise, they are removed from images and success of segmentation reduces. In this study, adaptive threshold is applied using Gaussian windows. Thus, deletion of capillaries is prevented by examining image into small areas. After adaptive threshold process using Gaussian windows, some noise has not been deleted from the image.

Then, image sharpening is applied to make blood vessels more prominent. These noise may be able to eliminate a harder noise reduction algorithms. But, capillaries are damaged and vessel geometry is disturbed. For this reason, noise removal process must be done softly. 2D wiener filter is applied to remove noise, again. The window size of wiener filter is selected 3x3. After wiener filter is applied on image, undesired colors between black and white occur. In order to overcome these values, the threshold should be applied to image once again. For this reason, Otsu threshold method is applied. Blood vessels and noise are separated. The noise remained independent of vessel in non-vascular areas. The structure and thickness values of noise are smaller and more irregular than vessels. Therefore morphological opening process is used. Finally, circle which is located of the edges on blood vessels are removed. Flowchart of the proposed algorithm is shown in Fig. 1.

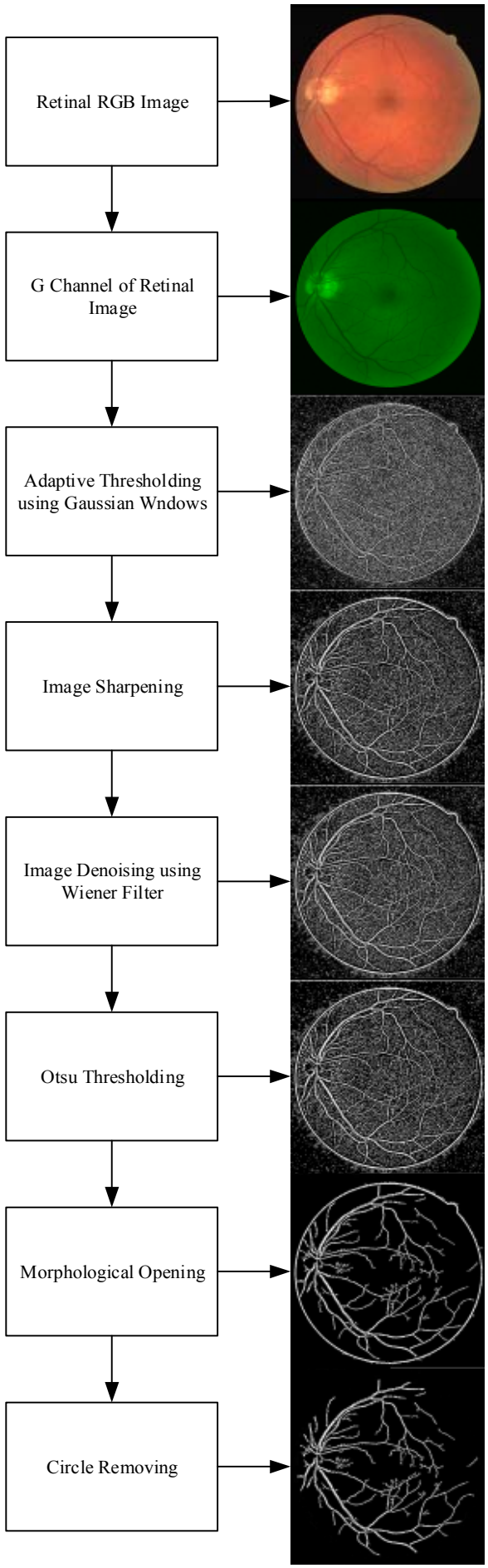

Figure 1 Structure of Proposed Method

A. Green Channel of Retinal Image:

Color fundus images contain red, green and blue color bands in certain proportions. Each of these bands include various features related to image. The green band has the cleanest data related to the blood vessels in retinal image. The green channel information are obtained by using Eq. 1.

$$Gr(x,y)=I(x,y,2) \quad (1)$$

where *Gr(x,y)* is green band of retinal image, *I(x,y,2)* is the part where green color components of color retinal image. *x* and *y* represent rows and columns, respectively. In color image, *I(x,y,1)* contains red band information, *I(x,y,2)* contains green band information and *I(x,y,3)* contains blue band information. Obtained green band is shown in Fig. 2.

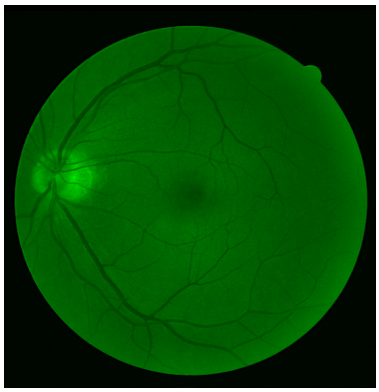

Figure 2. Green channel image

B. Adaptive Thresholding Using Gaussian Windows:

If an image have different brightness values in different regions, adaptive threshold should be applied. In adaptive threshold methods, image is generally evaluated by dividing small pixel groups. A threshold value is selected for each pixel group. If center pixel is greater than threshold value, it is classified as white. In other cases, it is classified as black. In this study, Gaussian windows are used for adaptive thresholding. It has been very effective for noisy image thresholding. Gaussian window size is selected 5x5. So, gaussian value is calculated for 5x5 neighborhood of each pixel and this value becomes threshold value for center pixel. Eq. 2 is used for thresholding with Gaussian windows [19].

$$G(x,y)=\frac{1}{2\pi\sigma^2}e^{-\frac{x^2+y^2}{2\sigma^2}} \quad (2)$$

in which *G(x,y)* is Gaussian window, σ represents amplitude factor, *x* and *y* represent distance in pixels from center pixel. Created Gaussian windows are moved in image and convolution is performed. Local adaptive threshold result using Gaussian windows is shown in Fig. 3.

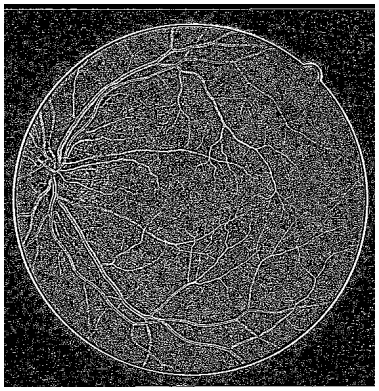

Figure 3. Adaptive thresholding using Gaussian windows

C. Image Sharpening:

After threshold process with Gaussian window, blood vessels in retinal image loses clarity. Image must be sharpened in order to clarify blood vessels. Sharpening process is carried out in *Lab* color space. Firstly, *RGB* color space is transformed into *XYZ* color space according to CIE 1931 standards. Eq. 3 is used for this color space transformation [20].

$$\begin{bmatrix} R \\ G \\ B \end{bmatrix} = \begin{bmatrix} 0.4184 & -0.1586 & -0.0828 \\ -0.0911 & 0.2524 & 0.0157 \\ 0.0009 & -0.0025 & 0.1786 \end{bmatrix} . \begin{bmatrix} X \\ Y \\ Z \end{bmatrix} \quad (3)$$

Then, *XYZ* color space is transformed to *Lab* color space. For this, Eq. 4, Eq. 5 and Eq. 6 are used.

$$L=100\sqrt{Y/Y_n} \quad (4)$$

$$a=172.3\left(\frac{X/X_n-Y/Y_n}{\sqrt{Y/Y_n}}\right) \quad (5)$$

$$b=67.2\left(\frac{Y/Y_n-Z/Z_n}{\sqrt{Y/Y_n}}\right) \quad (6)$$

where *L* represent luminance value, *a* represent green and magenta values, *b* represent yellow and blue values, Y_n, X_n and Z_n represent tristimulus values. *L* band is used for sharpening process. The main aim of increment in difference between pixels in *L* band is to provide high specificity for next stage. 3x3 sharpening filter which is used for sharpening is shown in Fig. 4.

-1	-1	-1
-1	9	-1
-1	-1	-1

Figure 4. Sharpening Template

The sharpening filter is applied to *L* band. Finally, it is converted to *RGB* color space. The image that occurs as a result of sharpening process is shown in Fig. 5.

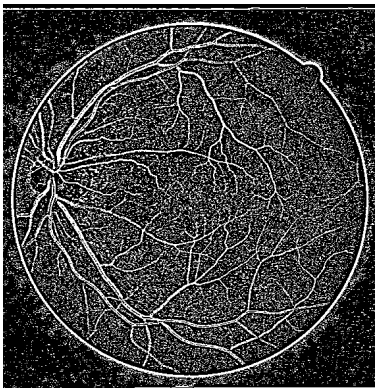

Figure 5. Sharpened Retinal Image

D. Image Denoising Using Wiener Filter:

After the sharpening process, some noise in image can be sharpened. In this case, blood vessels and noise cannot be distinguished. To avoid this undesired situation, irregularity feature of noise is used. An adaptive filter can remove noise without damaging vessel. Two dimensional Wiener filter is used for adaptive noise removal in this study. It obtains statistical feature of gray level image according to determined neighborhood value. It removes local mean and standard deviation of pixel neighborhood. If variance of pixel neighborhood is large, smaller smoothing is implemented by wiener filter. If variance of pixel neighborhood is small, more smoothing is applied on images by wiener filter. Image resulting from application of Wiener filter is shown in Fig. 6.

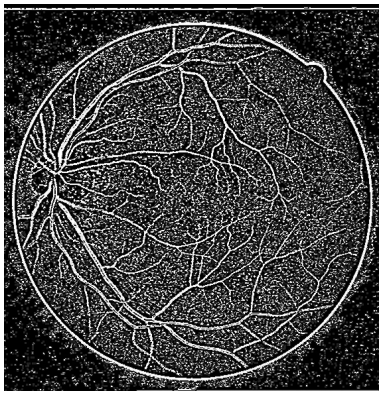

Figure 6. Image Denoising using Wiener Filter

E. Otsu Thresholding:

When wiener filter is cleaning image, it softens noise in some areas. Therefore, gray level values between white and black are occurred. Threshold should be done to eliminate these gray level values. For this, Otsu thresholding method [20] has been applied to the image. Firstly, threshold values are determined in the Otsu threshold method. In this study, one threshold value is applied for separating image into two classes. The image is divided into two classes called as C_0 and C_1. For this, probability distribution is calculated as Eq. 7.

$$P_i = h(i)/N \tag{7}$$

where *h(i)* represent pixel number and *N* represent totally number of pixel. Gray level possibilities are summed in themselves for C_0 *and* C_1 and the weight of each cluster is calculated as Eq. 8;

$$W_0 = \sum_{i=0}^{t-1} P_i \qquad W_1 = \sum_{i=t}^{L-1} P_i \tag{8}$$

The average values of clusters are calculated as Eq. 9;

$$\mu_0 = \sum_{i=0}^{t-1} \left(\frac{i.P_i}{W_0} \right) \qquad \mu_1 = \sum_{i=t}^{L-1} \left(\frac{i.P_i}{W_1} \right) \tag{9}$$

The average density value of the entire image is computed as Eq. 10;

$$\mu_t = \mu_0 W_0 + \mu_1 W_1 \tag{10}$$

The variances of classes are calculated as Eq. 11;

$$\sigma_0 = W_0 (\mu_0 - \mu_t)^2 \qquad \sigma_1 = W_1 (\mu_1 - \mu_t)^2 \tag{11}$$

The objective function for Otsu method is calculated using Eq. 12.

$$f(t) = \sigma_0 + \sigma_1 \tag{12}$$

Finally, threshold value which maximizes objective function is found. Image that is formed after thresholding process is shown in Fig. 7.

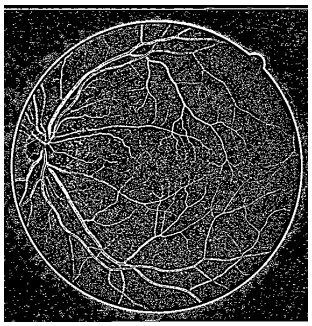

Figure 7. Retinal image after Otsu thresholding

F. Morphological Opening:

The blood vessels are classified as white and background is classified as black thanks to thresholding process. But, some noise still exist in image. These noises are classified as white, too. It must be removed from image. For this, structural differences between noise and blood vessels are examined. In retinal image, noise is smaller pixel groups than vessel pixel groups and it has irregular structure. These noise can be cleaned using morphological opening by using these features. Eq. 13 is used for morphological opening operation.

$$X \circ B = (X \ominus B) \oplus B \tag{13}$$

where *X* represents image, *B* represents structural element. In morphological opening process, only noise is deleted because blood vessels and noise do not contact each other. Blood vessels' image is shown in Fig. 8.

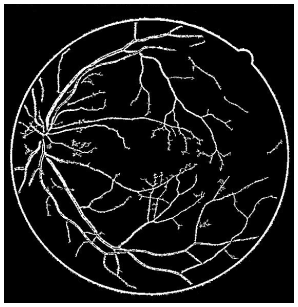

Figure 8. Blood vessels image after morphological opening

G. Circle Removing:

A circular shape is formed in image because of fundus camera limits. Finally these shape is removed. For this, shape is determined using Hough transform and it is removed in image. Retinal image blood vessel image is shown in Fig. 9.

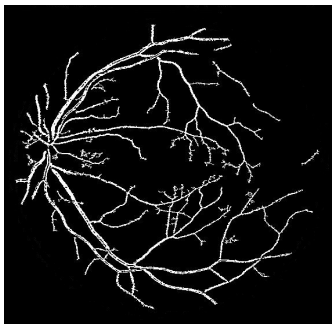

Figure 9. Retinal image blood vessels

III. Implementation Of Proposed Algorithm

Implementation results and performance results of proposed algorithms are described in section III. The proposed algorithm is tested using DRIVE dataset. 20 pieces test image in DRIVE dataset are used. Size of these images are 565x584 pixel. Proposed algorithm is implemented on a computer with an Intel Core i5-5200u (2.7 GHz) and 3 GB RAM. Implementation results of proposed algorithm are shown in Fig. 10.

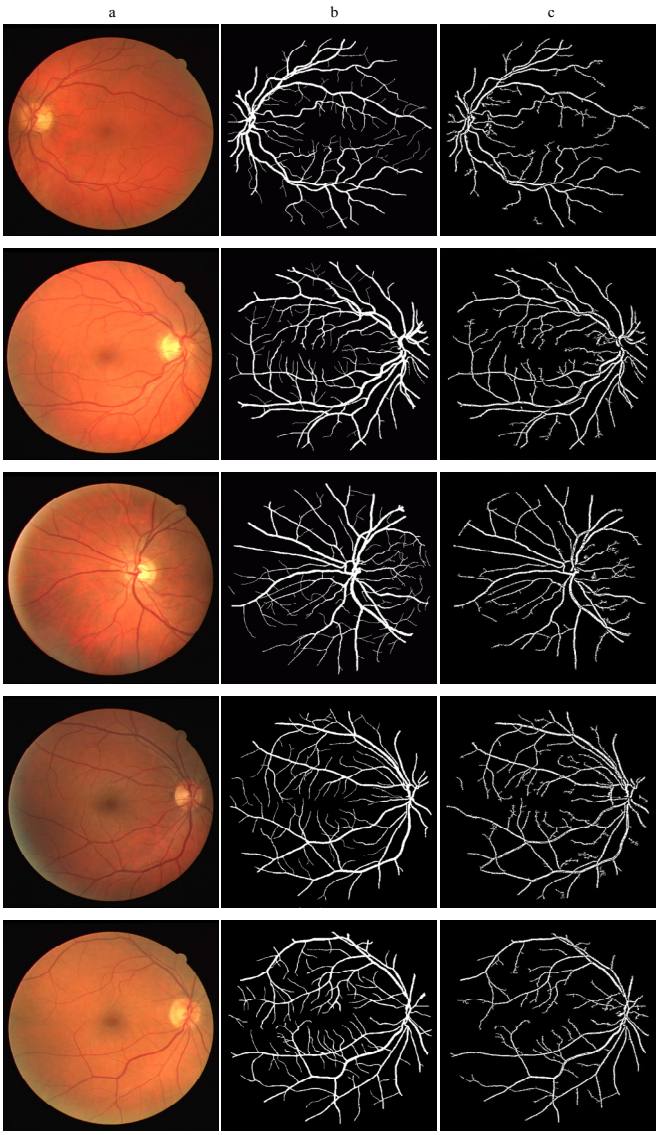

Figure 10 Implementation of Proposed Algorithm a) original image, b) reference image, c) segmented image using proposed algorithm

Sensitivity, specificity and accuracy values of proposed system are calculated to measure performance. Eq. 14, Eq. 15 and Eq. 16 are used, respectively.

$$Sensivity = \frac{TP}{TP + FN} \tag{14}$$

$$Specificity = \frac{TN}{TN + FP} \tag{15}$$

$$Accuracy = \frac{TP + TN}{TP + TN + FP + FN} \tag{16}$$

where *TP* is correctly identified number of total white pixel, *FP* is incorrectly identified number of total white pixel number, *TN* is correctly defined as total black pixel number, *FN* is incorrectly represented as total black pixel number. Table 1 shows that proposed algorithm results for each retinal image.

TABLE 1. PERFORMANCE EVALUATION OF PROPOSED ALGORITHM

	Sensitivity (%)	Specificity (%)	Accuracy (%)
01_test	83.17	97.13	96.11
02_test	90.11	96.49	96
03_test	83.36	96.26	95.42
04_test	87.37	96.71	96.10
05_test	87.93	96.92	96.39
06_test	91.24	95.60	95.35
07_test	85.52	95.83	95.20
08_test	78.87	95.70	94.73
09_test	91.13	96.04	95.81
10_test	82.65	96.46	95.64
11_test	83.27	97.13	96.19
12_test	81.76	96.93	95.98
13_test	88.75	95.10	94.70
14_test	78.81	97	95.78
15_test	68.55	97.42	95.29
16_test	89.07	96.28	95.83
17_test	85.22	95.99	95.40
18_test	88.99	96.10	95.65
19_test	87.52	96.05	95.44
20_test	88.63	95.66	95.25
Average	85.096	96.33	95.61

The obtained results are compared with results of other studies performed on DRIVE dataset. Comparison results can be seen in Table 2.

TABLE 2. COMPARISON OF PROPOSED ALGORITHM

Method	Process Time	Computer Specifications	Software
Mendonça [6]	2.5 to 3 mins	Pentium-4 . 3.2 GHz. 960 Mb RAM	MATLAB
Lam [7]	13 mins	Duo CPU 1.83 GHz. 2.0 GB RAM	MATLAB
Al-Diri [8]	11 mins	—	MATLAB
Strisciuglio [11]	60 s	—	MATLAB
Soares [15]	27.5 s	—	MATLAB
Li [18]	1.2 min	—	MATLAB
Proposed	**0.7- 0.8 s**	**Intel Core i5-5200u (2.7 GHz) and 3 GB RAM.**	**MATLAB**

The blood vessels geometry results of proposed method are more distinct. It is an unsupervised method which has low computational complexity. Therefore, system response is in range of 0.7-0.8 seconds as Table 3.

TABLE 3. COMPARISON OF COMPUTATIONAL PERFORMANCES

Type	Method	Sensitivity (%)	Specificity (%)	Accuracy (%)
Unsupervised	Mendonca [6]	73.44%	97.64%	94.63%
	Lam [7]	72.82%	95.51%	-
	Al-Diri [8]	-	-	94.72%
	Roychowdhury [9]	73.95%	97.82%	94.94%
	Nguyen [10]	73.22%	96.59%	94.07%
	Strisciuglio [11]	77.31%	97.24%	94.67%
	Proposed Algorithm	**85.096%**	96.33%	**95.61%**
Supervised	Soares [15]	73.32%	97.82%	94.66%
	You [16]	74.10%	97.50%	94.30%
	Fraz [17]	74.06%	94.80%	94.80%
	Li [18]	74.06%	**98.16%**	95.27%

IV. CONCLUSIONS

In this paper, fast and effective unsupervised retinal blood vessel segmentation method is presented. Proposed method based on thresholding and morphological operations. A general purpose is to segment blood vessels by eliminating background noise. It is tested using 20 test images on the DRIVE dataset. Blood vessel geometry of segmented images is quite successful. Also, process time of it is between 0.7-0.8s. Compared to other supervised and unsupervised algorithms it works pretty fast. So, it can be used real time computer aided diagnosis. Considering 85.096% sensitivity, 96.33% specificity and 95.61% accuracy results, sensitivity value of proposed method are more successful than other unsupervised algorithms. Sensitivity value is very important for success criteria of algorithms because it indicates percentage of white pixels correctly classified. In future, segmented images which are obtained from proposed method will be used to diagnose diseases such as hypertension and diabetic retinopathy.

REFERENCES

[1] Q. Li, B. Feng, L. Xie, P. Liang, H. Zhang, and T. Wang, "A Cross-Modality Learning Approach for Vessel Segmentation in Retinal Images," IEEE Transactions on Medical Imaging, vol. 35, no. 1, pp. 109–118, 2016. doi: 10.1109/TMI.2015.2457891.

[2] C. Kirbas and F. Quek, "A review of vessel extraction techniques and algorithms," ACM Computing Surveys, vol. 36, no. 2, pp. 81–121, Jan. 2004. doi: 10.1145/1031120.1031121.

[3] International Diabetes Federation. "IDF diabetes atlas-7th edition". http://www.diabetesatlas.org. 2016-3-10.

[4] U. T. Nguyen, A. Bhuiyan, L. A. Park, and K. Ramamohanarao, "An effective retinal blood vessel segmentation method using multi-scale line detection," Pattern Recognition, vol. 46, no. 3, pp. 703–715, 2013. doi: 10.1016/j.patcog.2012.08.009.

[5] J. Staal, M. Abramoff, M. Niemeijer, M. Viergever, and B. V. Ginneken, "Ridge-Based Vessel Segmentation in Color Images of the Retina," IEEE Transactions on Medical Imaging, vol. 23, no. 4, pp. 501–509, 2004. doi: 10.1109/tmi.2004.825627.

[6] A. Mendonca and A. Campilho, "Segmentation of retinal blood vessels by combining the detection of centerlines and morphological reconstruction," IEEE Transactions on Medical Imaging, vol. 25, no. 9, pp. 1200–1213, 2006. doi: 10.1109/tmi.2006.879955.

[7] B. S. Y. Lam, Y. Gao, and A. W.-C. Liew, “General Retinal Vessel Segmentation Using Regularization-Based Multiconcavity Modeling,” IEEE Transactions on Medical Imaging, vol. 29, no. 7, pp. 1369–1381, 2010. doi: 10.1109/tmi.2010.2043259.

[8] B. Al-Diri, A. Hunter, and D. Steel, “An Active Contour Model for Segmenting and Measuring Retinal Vessels,” IEEE Transactions on Medical Imaging, vol. 28, no. 9, pp. 1488–1497, 2009. doi: 10.1109/tmi.2009.2017941.

[9] S. Roychowdhury, D. Koozekanani and K. Parhi, “Iterative Vessel Segmentation of Fundus Images,” IEEE Trans. Bio. med. Eng., vol. 62. no. 7, pp. 1738–1749, 2015. doi: 10.1109/TBME.2015.2403295.

[10] N.U. TV, A. Bhuiyan, L.A. Park and K. Ramamohanarao, "An Effective Retinal Blood Vessel Segmentation Method Using Multi-Scale Line Detection," Pattern recognition, vol. 46, no. 3, pp. 703-715, 2013. doi:10.1016/j.patcog.2012.08.009.

[11] A. George, N. Strisciuglio, M. Vento and N. Petkov, "Trainable COSFIRE Filters For Vessel De-Lineation with Application to Retinal Images," Medical image analysis, vol. 19, no. 1, pp. 46-57, 2015. doi: 10.1016/j.media.2014.08.002.

[12] B. Yin, H. Li, B. Sheng, X. Hou, Y. Chen, W. Wu, P. Li, R. Shen, Y. Bao and W. Jia, “Vessel Extraction From Non-Fluorescein Fundus Images Using Orientation-Aware Detector,” Med. Image Anal., vol. 26, no. 1. pp. 232–242, 2015. doi: 10.1016/j.media.2015.09.002.

[13] Z. Jingdan, Y. Cui, W. Jiang and L. Wang, "Blood Vessel Segmentation of Retinal Images Based on Neural Network," In International Conference on Image and Graphics, pp. 11-17, 2015. doi:10.1007/978-3-319-21963-9_2.

[14] S. Nicola., G. Azzopardi, M. Vento and N.Petkov, “Multiscale Blood Vessel Delineation Using B-COSFIRE Filters,” In International Conference on Computer Analysis of Images and Patterns, pp. 300-312, 2015. doi: 10.1007/978-3-319-23117-4_26.

[15] J.V. B. Soares, J. J. G.Leandro, R. M. C. Júnior and M.J. Cree, "Retinal Vessel Segmentation Using The 2-D Gabor Wavelet and Supervised Classification," IEEE Transactions on medical Imaging, vol. 25, no. 9, pp. 1214-1222, 2006. doi: 10.1109/TMI.2006.879967.

[16] Y. Xinge, Q. Peng, Y. Yuan, Y. Cheung and J. Lei, "Segmentation of Retinal Blood Vessels Using The Radial Projection And Semi-Supervised Approach," Pattern Recognition, vol. 44, no. 10, pp. 2314-2324, 2011. doi: 10.1016/j.patcog.2011.01.007.

[17] M. Fraz, P. Remagnino, A. Hoppe, B. Uyyanonvara, A. Rudnicka, C. Owen and S. Barman, “An Ensemble Classification-Based Approach Applied To Retinal Blood Vessel Segmentation,” IEEE Trans. Biomed. Eng., vol. 59, no. 9, pp. 2538–2548, 2012. doi:10.1109/TBME.2012.2205687

[18] Q. Li, B. Feng, L. Xie, P. Liang, H. Zhang and T. Wang, “A Cross Modality Learning Approach for Vessel Segmentation in Retinal Images,” IEEE Trans. Med. Imag., vol. 35, no. 1, pp. 109–118, 2016. doi: 10.1109/TMI.2015.2457891.

[19] L. Gang, O. Chutatape, S. M. Krishnan, “Detection and Measurement of Retinal Vessels in Fundus Images Using Amplitude Modified Second-Order Gaussian Filter,” IEEE transactions on Biomedical Engineering, vol. 49, no. 2, pp. 168-172, 2002. doi: 10.1109/10.979356.

[20] C. L. Lin and C. Y. Su, “Modified unsharp Masking Detection Using Otsu Thresholding and Gray Code,” In 2016 IEEE International Conference on Industrial Technology (ICIT), pp. 787-791, 2016. doi: 10.1109/ICIT.2016.7474851.

View publication stats